Weakly bound and strained C_{60} monolayer on the Si(111) $\sqrt{3}\times\sqrt{3}R30°$-Ag substrate surface

T. Nakayama,* J. Onoe, and K. Takeuchi
The Institute of Physical and Chemical Research (RIKEN), 2-1 Hirosawa, Wako, Saitama 351-01, Japan

M. Aono
The Institute of Physical and Chemical Research (RIKEN), 2-1 Hirosawa, Wako, Saitama 351-01, Japan
and Department of Precision Science and Technology, Osaka University, Suita, Osaka 565, Japan
(Received 30 November 1998; revised manuscript received 29 January 1999)

Using scanning tunneling microscopy, we observed the growth and structure of a C_{60} monolayer on a Si(111) $\sqrt{3}\times\sqrt{3}R30°$-Ag substrate at room temperature, and found various C_{60} arrangements with different strain fields in a molecularly flat C_{60} monolayer. The results are understood by two kinds of molecule-substrate interactions, a weak interaction on the terrace and a strong interaction at the step of the substrate. The weak interaction may not be a pure van der Waals interaction, and the binding energy of a single C_{60} molecule on the Si(111) $\sqrt{3}\times\sqrt{3}R30°$-Ag surface is surmised to be 0.8–0.9 eV. The probability of defect appearance in the C_{60} monolayer increases when the strain energy increases, and a highly ordered defect arrangement is realized probably due to the effective release of strain energy. [S0163-1829(99)11119-6]

I. INTRODUCTION

In order to investigate the nature of C_{60} films by scanning tunneling microscopy (STM), conductive substrates such as metals or semiconductors are required. On the other hand, it is known that C_{60} molecules interact strongly with metal and semiconductor substrates[1,2] except for GaAs(110).[3,4] The strong interaction between the molecule and the substrate generally overcomes the intermolecular van der Waals interaction.[5] For example, highly strained C_{60} film can be stabilized on Au(001) due to a strong molecule-substrate interaction.[6] In the case of C_{60} on GaAs(110), commensurate C_{60} monolayers are formed at room temperature (RT).[3] In the commensurate C_{60} monolayer on GaAs(110), C_{60} molecules can adsorb at two different sites,[3] and this causes the rippling structure of the monolayer. The rippling of C_{60} molecules seems to reduce the strain energy due to a small intermolecular distance of 0.98 nm that has been measured along the surface parallel direction.

In this paper, we show the growth and structure of a C_{60} monolayer on a Si(111) $\sqrt{3}\times\sqrt{3}R30°$-Ag substrate[7–13] at room temperature. The Si(111) $\sqrt{3}\times\sqrt{3}R30°$-Ag substrate allows formation of a very flat and weakly bound C_{60} monolayer.[14] A variety of intermolecular distances have been found in the C_{60} monolayer, in contrast to the previous STM study,[14] resulting in various strain fields. We discuss the probability of defect appearance and the arrangement of defects in the C_{60} monolayer that is related to the strain energy.

II. EXPERIMENT

The Si(111) $\sqrt{3}\times\sqrt{3}R30°$-Ag substrates were prepared by depositing one monolayer (7.83×10^{14} atoms/cm^2) of Ag onto clean Si(111) surfaces according to a procedure described elsewhere.[15] C_{60} molecules were thermally evaporated from a pyrolitic boron nitride crucible supported in a tungsten basket heated with a fixed dc current and deposited onto the substrate at room temperature for 3 min. This resulted in a reproducible amount of C_{60} deposition. All the above procedures were done in an ultra-high-vacuum (UHV) chamber with a maximum pressure of around 1×10^{-7} Pa. The STM observations were performed at room temperature in UHV below 1×10^{-8} Pa. We used both platinum–20% irridium and tungsten tips.

The rates of C_{60} growth were clearly dependent on the step density of the substrate. Therefore, we controlled the step density of the substrate by changing temperatures of the clean Si(111) surface,[15] within a range of 350 to 550 °C, when Ag atoms are deposited onto it. We note that such step density is not only dependent on the above substrate preparation condition, but also on the local flatness of the substrate.

Since the surface structure of Si(111) $\sqrt{3}\times\sqrt{3}R30°$-Ag (Refs. 8 and 9) and the corresponding STM images[10,11] are well understood as a result of previous extensive studies, we used the substrate as a scale to measure the intermolecular distances. Although there was uncertainty in determining the position of individual C_{60} molecules due to their relatively large size (around 1 nm in diameter in each STM image), by averaging more than 200 equivalent intermolecular distances, we could achieve errors of ±0.009 nm at maximum.

III. RESULTS

A. Structure of C_{60} monolayer

The first C_{60} monolayer involves various domains with different structures, though the Si(111) $\sqrt{21}\times\sqrt{21}R10.9°$-(Ag, C_{60}) phase[14] (referred to as the $\sqrt{21}$-(Ag, C_{60}) phase, hereafter) is a thermal equilibrium phase, as will be described later. Figures 1(a) and 1(b) show two different domains adjacent to the Si(111) $\sqrt{3}\times\sqrt{3}R30°$-Ag structure. In Fig. 1(a), positions of the C_{60} molecules are registered with respect to the underlying sub-

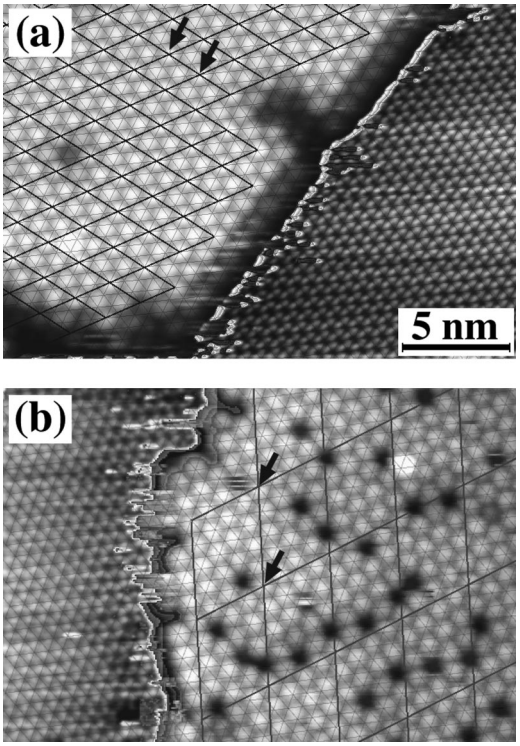

FIG. 1. STM images of the (a) $\sqrt{21}$-(Ag, C_{60}) domain with hexagonal molecular arrangement and (b) the other domain with distorted hexagonal molecular arrangement. Shown is a superimposed lattice where thin and thick solid lines represent the periodicity of the substrate and C_{60} adsorbed structures, respectively. The contrast of the substrate regions [right- and left-hand sides of the images in (a) and (b), respectively] were enhanced for clarity.

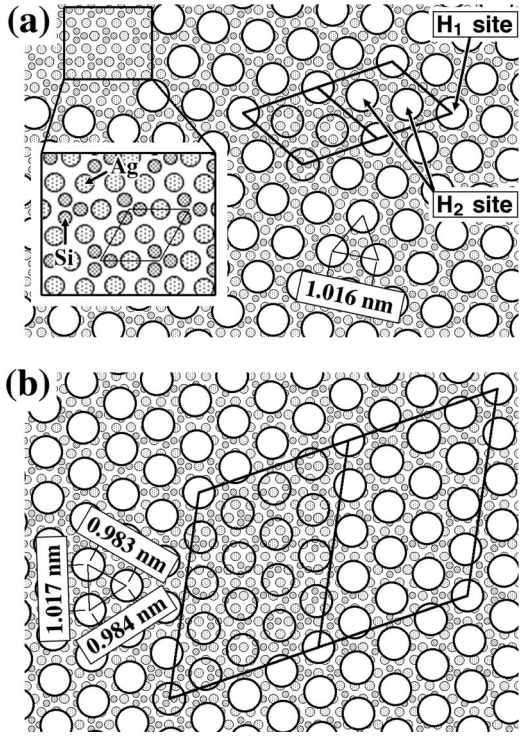

FIG. 2. Structure models for the observed C_{60} arrangements. Models shown in (a) and (b) correspond to the molecular arrangements observed in Figs. 1(a) and 1(b), respectively. White and transparent circles represent C_{60} molecules and the others are Ag and Si atoms, as indicated in (a).

strate structure, using a superimposed lattice (thin solid lines). The C_{60} molecules, indicated by arrows in both figures, occupy equivalent sites. The corresponding unit lattices are drawn by thick lines in the figures. The molecular arrangement in Fig. 1(a) corresponds to the $\sqrt{21}$-(Ag, C_{60}) phase and that observed in Fig. 1(b) does not coincide with that in Fig. 1(a). We note that the registration in Fig. 1(b) is not perfect, as seen at the boundary of the image. The unit lattice in Fig. 1(b) is the one that can fit the widest area of the C_{60} domain, meaning that this domain is incommensurate with the substrate. The different densities of defects observed in these domains will be discussed later.

The models for Figs. 1(a) and 1(b) are schematically drawn in Figs. 2(a) and 2(b), respectively. Although there are many missing-molecule defects observed in Fig. 1(b), they are neglected in Fig. 2(b). The molecular arrangement in Fig. 2(a) shows a complete hexagonal packing of C_{60} molecules with an intermolecular distance of 1.016 nm, which involves two kinds of C_{60} adsorbates, as indicated by H_1 and H_2. The type H_1 molecule is located on top of the Si trimer of the $\sqrt{3}$-Ag structure; the type H_2 molecule is located on the middle of the three neighboring Ag trimers.[8,9] The C_{60} molecules in Fig. 2(b) are arranged in a slightly distorted hexagonal fashion with three intermolecular distances of 1.017, 0.984, and 0.983 nm, as shown in the figure. The statistical error in these values, arising from the incommensuration mentioned above, is ± 0.009 nm.

We have obtained many STM images that show the coexistence of various structures in the first C_{60} monolayer, an example of which is shown in Fig. 3. In this STM image, there are six C_{60} monolayer domains, as indicated by A–F. Domains F' and F are equivalent and related by a translational phase shift. Domains A–D are 0.314 nm lower than domains E, F, and F' due to a substrate step. The Si(111) $\sqrt{3}\times\sqrt{3}R30°$-Ag substrate surface is a single do-

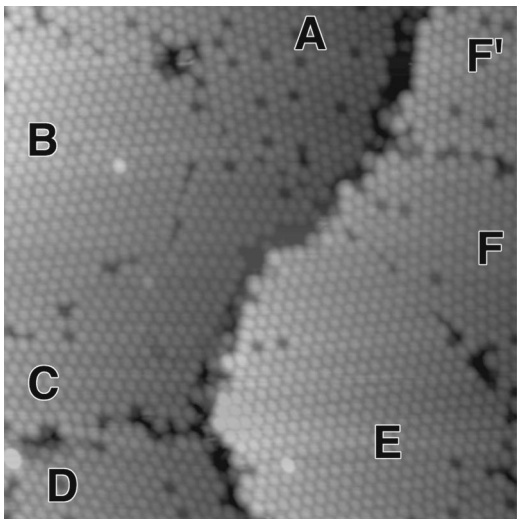

FIG. 3. STM image showing coexistence of six domain structures. Note that domain F' is equivalent to F and that domains A–D are 0.314 nm lower in height than E–F' due to a substrate step.

main surface if we exclude translational phase shifts,[15] so the $\sqrt{21}$-(Ag, C_{60}) phase can realize only two domains[14] on this substrate. The present result, however, clearly shows the coexistence of six domains. An interesting finding is that all the structures observed in the first C_{60} monolayer are molecularly flat, in contrast to the case of C_{60} grown on GaAs(110).[3]

We note that the $\sqrt{21}$-(Ag, C_{60}) phase dominates the monolayer structure when we slightly anneal the sample. For example, two annealing conditions, $\sim$100 °C for 10 h and $\sim$200 °C for 3 min, resulted in a domination of the surface with the $\sqrt{21}$-(Ag, C_{60}) phase. Increasing the substrate temperature to about 250 °C for several minutes resulted in the removal of C_{60} molecules from the substrate terraces, which is consistent with a previous STM study.[14]

B. Defects in C_{60} monolayer

Strain fields can be generated depending on the arrangement of C_{60} in a domain. Since the optimum intermolecular distance between two C_{60} molecules is 1.005 nm,[5] longer and shorter intermolecular distances will cause tensile and compressive strain, respectively. In strained domains, we observed missing-molecule defects. For example, the domain observed in Fig. 1(a) is almost perfect, while that in Fig. 1(b) contains many missing-molecule defects. Similarly, domains in Fig. 3 also have different densities of missing-molecule defects: domain *B* has no defect, while domain *A* does have defects, for example. When we define the probability of defect appearance as the number of defects divided by the number of C_{60} molecules observed in a domain, the probability in the domain shown in Fig. 1(b) is 0.127 (we used another STM image that observed a larger area of the same domain).

Further deposition of C_{60} onto the sample shown in Figs. 1(a) and 1(b) yields a second C_{60} layer, as shown in Fig. 4(a). Interestingly, the probability of defect appearance increased after the growth of the second C_{60} layer. Here we again observed the substrate region adjacent to the monolayer region, as indicated in Fig. 4; we tried to registrate the adsorption sites of C_{60} molecules. Similar to the case of Fig. 1(b), perfect registration was again difficult. Therefore, the arrangement of the C_{60} molecules involves uncertainty due to the incommensuration as in Fig. 1(b). Intermolecular distances between C_{60} molecules in this domain were 1.071, 0.995, and 0.947 nm ($\pm$0.008 nm) and the probability of defect appearance was 0.207. The shortest intermolecular distance of 0.947 nm should cause large compressive strain in the domain. In the case of such a high probability of defect appearance, we find that the defects have a certain ordering. The defect arrangement in the rectangle in Fig. 4(a) is schematically reproduced in Fig. 4(c), where the molecules and defects are represented by open and closed circles, respectively.

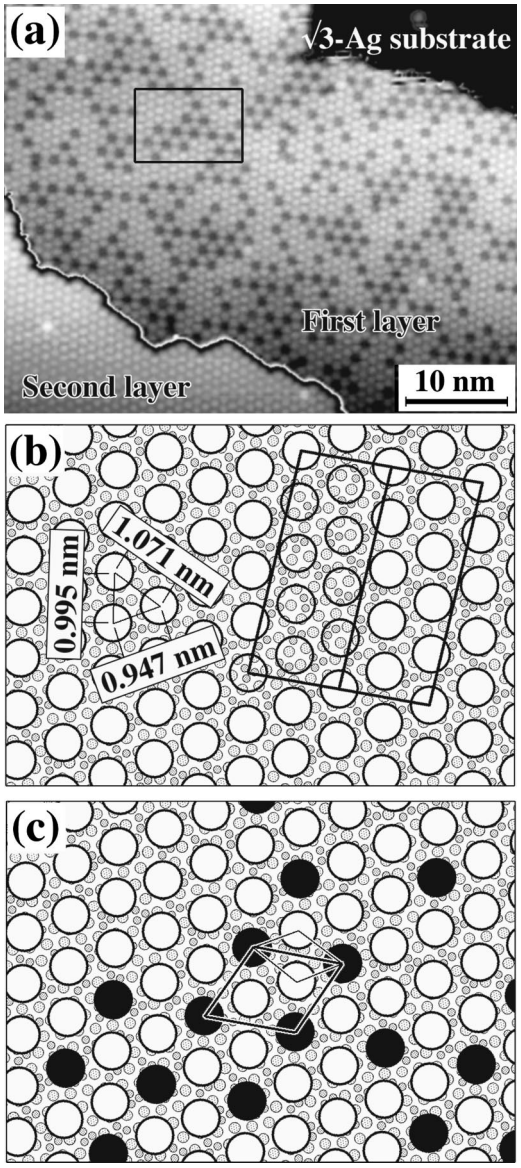

FIG. 4. (a) STM image of the first C_{60} monolayer having a high density of defects, (b) C_{60} arrangement in the first monolayer in (a), (c) schematic drawing of the defect arrangement observed in the rectangular region indicated in (a). In (c), solid circles represent defect and the periodicity of the defect arrangement is also shown.

IV. DISCUSSION

The desorption temperature of $\sim$250 °C is close to those observed in the cases of multilayered C_{60} films (233–333 °C),[16,17] indicating that the desorption energy for C_{60} adsorbed on Si(111) $\sqrt{3}\times\sqrt{3}R30°$-Ag is almost the same as the case of multilayered C_{60} films. Wang *et al.*[18] has shown, using an STM, that the multilayered C_{60} film is not amorphous, but almost a single-crystalline film. Since a single C_{60} molecule on a flat C_{60} terrace of (111) facet is bound to three underlying C_{60} molecules, the binding (adsorption) energy of a single molecule on a flat terrace of the multilayered C_{60} film becomes 0.83 eV, as readily calculated from the Girifalco potential,[5] a modified Lennard-Jones potential taking the spherical shape of the C_{60} molecule into account. As mentioned in a previous paper,[16] this binding energy deviates considerably from the measured desorption energy. Under these considerations, we surmise that the binding energy of a single C_{60} molecule on the Si(111) $\sqrt{3}\times\sqrt{3}R30°$-Ag surface structure is similar to the case of the multilayered C_{60} film, being 0.8–0.9 eV.

We observed various structures in the first C_{60} monolayer,

and the most stable structure seems to be the $\sqrt{21}$-(Ag,C_{60}) phase, as mentioned already. The coexistence of various structures found in our experiments is in contrast to the double domain ordering reported in a previous experiment.[14] This difference may be due to the kinetic conditions in the growth of C_{60} layers. The saturation coverage was estimated to be about one molecular layer for 3 min deposition, so the deposition rate was ~0.33 molecular layer per 1 min (ML/min) in this work while it was 0.05 ML/min in the previous work.[14] The structures that are not the most stable would remain because of a pinning effect at the step edge or at the boundaries between the C_{60} domains. Indeed, C_{60} molecules are strongly bound to the substrate steps,[14] and this may affect the molecular arrangements over domains if the molecule-substrate interaction is weak enough.

An additional insight related to the ''weak'' interaction between the C_{60} molecule and the substrate can be obtained by simply considering the following. If the molecule is completely physisorbed, we are able to estimate the possible height variation in the first C_{60} monolayer. By taking the van der Waals radii of Ag and Si to be 0.172 and 0.210 nm,[19] respectively, and by considering atomic coordinates of the Si(111)$\sqrt{3}\times\sqrt{3}$-Ag structure as resolved by surface x-ray diffraction experiments,[20] a ''van der Waals surface'' of the substrate can be derived. Although there is a 0.08 nm height difference between the center of the topmost Ag and that of the first Si layers in the $\sqrt{3}$-Ag structure, different van der Waals radii for Ag and Si make the surface very flat with a peak-to-peak roughness of 0.04 nm. A schematic representation for possible C_{60} adsorption is shown in Fig. 5(a). In this figure, high-symmetry adsorption sites of H_1, H_2 [the same as those in Fig. 2(a)], and T (on top of a topmost Ag atom) are selected to accommodate C_{60} molecules with a van der Waals radius of 0.5025 nm.[5] The C_{60} molecule at H_1 is the lowest, and those at H_2 and at T are 0.024 and 0.055 nm higher than the lowest molecule, respectively, so the height difference among the C_{60} molecules is a maximum of 0.055 nm.

Actually, the C_{60} monolayer is very flat, as we have discussed. The height variation of C_{60} molecules in the monolayer was below 0.04 nm in topographic STM images taken under various tunneling conditions. Figure 5(b) shows the variations in tip height over the C_{60} molecules in the $\sqrt{21}$-(Ag, C_{60}) phase. Four different curves were measured with different sample bias voltages, as indicated in the figure, and with a fixed tunneling current of 80 pA. As indicated in the figure, each peak corresponds to an individual C_{60} molecule located at H_1 or H_2. By comparing these measurements in light of the above simple consideration, we note that the expectation based on van der Waals interaction is not realized in the experiments; the C_{60} molecules at H_2 sites are apparently lower than those at H_1 sites, especially at negative sample bias voltages. This discrepancy presumably indicates the existence of a charge transfer between the molecule and the substrate, suggesting that the weak interaction between C_{60} and the substrate may not be a pure van der Waals interaction.

Finally, we discuss the effect of a strain field that exists in a domain with distorted hexagonal arrangement of C_{60}. Since the C_{60} monolayer is molecularly flat, it is reasonable

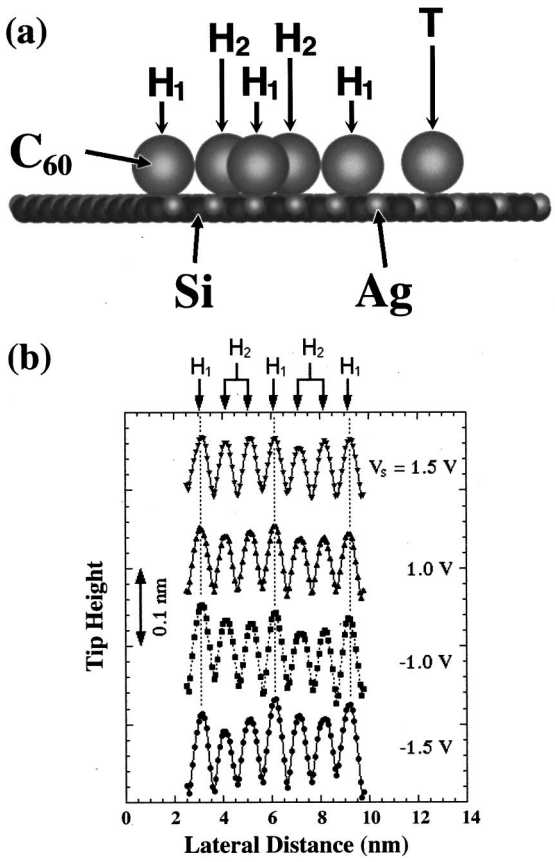

FIG. 5. (a) Van der Waals model of C_{60} on Si(111) $\sqrt{3}\times\sqrt{3}R30°$-Ag. (b) Tip height variation over the C_{60} molecules at H_1 and H_2 sites with different sample bias voltages.

to assume that the strain energy in a domain simply depends on the intermolecular distances measured by the STM. Here, the strain energy per single molecule is estimated on the basis of the Girifalco potential.[5] In the case of an ideal hexagonal arrangement with an intermolecular distance of 1.005 nm, the total binding energy of one C_{60} molecule surrounded by six other C_{60} molecules is calculated to be $1.66+E_b$ eV, where $E_b=0.8$–0.9 eV is the binding energy of an isolated C_{60} molecule on the substrate. When the ideal hexagonal arrangement is distorted, such as shown in Fig. 2(b) or 4(b), the strain energy of the C_{60} molecules is calculated to be 0.15 or 1.37 eV, respectively.

Higher strain energy generally results in a higher probability of defect appearance in our experiments. However, the difference in strain energies of 1.22 eV per molecule is too large to explain the difference in the probability of defect appearance (0.127 and 0.207), judging from the Boltzmann factor estimated at room temperature. Since we observed the periodic arrangement of defects in highly defective domains, the periodic arrangement seems to release strain energy more effectively than the case of random defect distribution.

V. SUMMARY

Using STM, we observed the growth and structure of a C_{60} monolayer on a Si(111)$\sqrt{3}\times\sqrt{3}R30°$-Ag substrate at

room temperature, and found various C_{60} arrangements with different strain fields in a molecularly flat C_{60} monolayer on the Si(111)$\sqrt{3}\times\sqrt{3}R30°$-Ag substrate. The results are understood by two kinds of molecule-substrate interactions, a weak interaction on the terrace and a strong interaction at the step of the substrate. The weak interaction may not be a pure van der Waals interaction, and the binding energy of a single C_{60} molecule on the Si(111)$\sqrt{3}\times\sqrt{3}R30°$-Ag surface is surmised to be 0.8–0.9 eV. The probability of defect appearance in the C_{60} monolayer increases when the strain energy increases, and a highly ordered defect arrangement is realized probably due to effective release of the strain energy.

ACKNOWLEDGMENTS

This work was partially supported by the Program of Core Research for Evolutional Science and Technology (CREST), Japan Science and Technology Corporation, and by special coordination funds of the Science and Technology Agency of the Japanese Government.

*Author to whom correspondence should be addressed. Electronic address: tomonobu@postman.riken.go.jp

[1] M.S. Dresselhaus, G. Dresselhaus, and P.C. Eklund, *Science of Fullerenes and Carbon Nanotubes* (Academic Press, San Diego, CA 1996), p. 712.
[2] T. Sakurai, Q. Xue, T. Hashizume, and Y. Hasegawa, J. Vac. Sci. Technol. B **15**, 1628 (1997).
[3] Y.Z. Li, J.C. Patrin, M. Chander, J.H. Weaver, L.P.F. Chibante, and R.E. Smalley, Science **252**, 547 (1991).
[4] Y.Z. Li, M. Chander, J.C. Patrin, J.H. Weaver, L.P.F. Chibante, and R.E. Smalley, Science **253**, 429 (1991).
[5] L.A. Girifalco, J. Phys. Chem. **96**, 858 (1992).
[6] Y. Kuk, D.K. Kim, Y.D. Suh, K.H. Park, H.P. Noh, S.J. Oh, and S.K. Kim, Phys. Rev. Lett. **70**, 1948 (1993).
[7] G. LeLay, Surf. Sci. **132**, 169 (1983).
[8] T. Takahashi, S. Nakatani, N. Okamoto, T. Ishikawa, and S. Kikuta, Jpn. J. Appl. Phys., Part 2 Part 2 **27**, L753 (1988).
[9] M. Katayama, R.S. Williams, M. Kato, E. Nomura, and M. Aono, Phys. Rev. Lett. **66**, 2762 (1991).
[10] Y.G. Ding, C.T. Chan, and K.M. Ho, Phys. Rev. Lett. **67**, 1454 (1991).
[11] S. Watanabe, M. Aono, and M. Tsukada, Phys. Rev. B **44**, 8330 (1991).
[12] K.J. Wan, X.F. Lin, and J. Nogami, Phys. Rev. B **47**, 13 700 (1993).
[13] A. Shibata, Y. Kimura, and K. Takayanagi, Surf. Sci. **303**, 161 (1994).
[14] M.D. Upward, P. Moriarty, and P.H. Beton, Phys. Rev. B **56**, R1704 (1997).
[15] T. Nakayama, S. Watanabe, and M. Aono, Surf. Sci. **344**, 143 (1995).
[16] A.V. Hamza and M. Balooch, Chem. Phys. Lett. **198**, 603 (1992).
[17] A.V. Hamza and M. Balooch, Chem. Phys. Lett. **201**, 404 (1993).
[18] X.-D. Wang, T. Hashizume, H. Shinohara, Y. Saito, Y. Nishina, and T. Sakurai, Phys. Rev. B **47**, 15 923 (1993).
[19] A. Bondi, J. Phys. Chem. **6**, 441 (1964).
[20] T. Takahashi and S. Nakatani, Surf. Sci. **282**, 17 (1993).